The β-Carboline Harmine Has a Protective Immunomodulatory Role in Nonhealing Cutaneous Leishmaniasis

Sanam Peyvandi[1], Qiang Lan[2], Antoine Chabloz[3], Florence Prével[1], Yazmin Hauyon La Torre[1], Annette Ives[3] and Fabienne Tacchini-Cottier[1]

Cutaneous leishmaniasis affects 1 million people worldwide annually. Although conventional treatments primarily target the parasite, there is growing interest in host immune modulation. In this study, we investigated the impact of synthetic β-carboline harmine (ACB1801), previously shown to be immunoregulatory in cancer, on the pathology caused by a drug-resistant *Leishmania major* strain causing persistent cutaneous lesions. Exposure to ACB1801 in vitro had a modest impact on parasite burden within host macrophages. Moreover, it significantly increased major histocompatibility complex II and costimulatory molecule expression on infected dendritic cells, suggesting an enhanced immune response. In vivo, ACB1801 monotherapy led to a substantial reduction in lesion development and parasite burden in infected C57BL/6 mice, comparable with efficacy of amphotericin B. Transcriptomics analysis further supported ACB1801 immunomodulatory effects, revealing an enrichment of TNF-α, IFN-γ, and major histocompatibility complex II antigen presentation signatures in the draining lymph nodes of treated mice. Flow cytometry analysis confirmed an increased frequency (1.5×) of protective $CD4^+$IFN-γ^+TNF-α^+ T cells and a decreased frequency (2×) in suppressive IL-10^+FoxP3^- T cells at the site of infection and in draining lymph nodes. In addition, ACB1801 downregulated the aryl hydrocarbon receptor signaling, known to enhance immunosuppressive cytokines. Thus, these results suggest a potential use for ACB1801 alone or in combination therapy for cutaneous leishmaniasis.

Keywords: AhR, Dendritic cells, Immunomodulator, *Leishmania*, Macrophages

Journal of Investigative Dermatology (2023) ■, ■–■; doi:10.1016/j.jid.2023.09.280

INTRODUCTION

Parasitic infections often use immune subversion to promote disease evolution and parasite persistence within the host. *Leishmania* are intracellular protozoan parasites causing leishmaniases, a group of neglected diseases with a clinical spectrum, including cutaneous, mucocutaneous, and the life-threatening visceral form (Mann et al., 2021). Some *Leishmania* spp can prevent or dampen host immune response by a multitude of immunosuppressive mechanisms, including impaired IFN-γ production by $CD4^+$ T cells and/or decreased activation of antigen-presenting cells, abrogating parasite control. Additional immunosuppression mechanisms include the secretion of the anti-inflammatory IL-10 cytokine by $CD4^+$ T cells in visceral (Bunn et al., 2018; Caldas et al., 2005) and in unhealing forms of cutaneous leishmaniasis (Lee et al., 2018). Regulation of the expression of major histocompatibility complex (MHC) molecules on antigen-presenting cells also influences protective host immune response in response to *Leishmania* infection. Immune checkpoint molecules, including PD-1 and CTLA-4, 2 negative regulators of infection, have also been observed on exhausted or anergic $CD4^+$ T cells in *Leishmania*-infected humans and mice (Costa-Madeira et al., 2022; de Freitas e Silva and von Stebut, 2021)

IFN-γ and TNF-α act synergistically to promote optimal microbicidal activation of macrophages. TNF downregulates ARG1 and thereby enhances the enzymatic activity of inducible nitric oxide synthase (iNOS) and nitric oxide production by macrophages for parasite killing. The balance between iNOS and arginase in macrophage activation is crucial for controlling the disease (Bogdan, 2020). The aryl hydrocarbon receptor (AhR) is a ubiquitously expressed protein with a crucial role in immunomodulation (Rothhammer and Quintana, 2019). AhR was shown to regulate TNF-α expression early after *Leishmania* infection and to regulate iNOS and arginase activity in macrophages, suggesting an important role in parasite control (Climaco-Arvizu et al., 2016; Elizondo et al., 2011; Münck et al., 2019).

New leishmaniasis treatments are needed because most treatments display toxic effects, and drug resistance is an

[1]*Department of Immunobiology, Faculty of Biology and Medicine, University of Lausanne, Epalinges, Switzerland;* [2]*Cell and Tissue Dynamics Research Program, Institute of Biotechnology, Helsinki Institute of Life Science (HiLIFE), University of Helsinki, Helsinki, Finland; and* [3]*AC BioScience SA, Epalinges, Switzerland*

Correspondence: Fabienne Tacchini-Cottier, Department of Immunobiology, Faculty of Biology and Medicine, University of Lausanne, 155, ch des Boveresses, Epalinges 1066, Switzerland. E-mail: Fabienne.Tacchini-Cottier@unil.ch

Abbreviations: AhR, aryl hydrocarbon receptor; BMDC, bone marrow–derived dendritic cell; BMDM, bone marrow–derived macrophage; DC, dendritic cell; dLN, draining lymph node; IDO, indoleamine 2,3-dioxygenase; iNOS, inducible nitric oxide synthase; i.p., intraperitoneally; LmSd, Leishmania major *Seidman; MHC, major histocompatibility complex; Th, T helper*

Received 11 July 2023; revised 15 September 2023; accepted 28 September 2023; accepted manuscript published online XXX; corrected proof published online XXX

ever-increasing challenge (eBioMedicine, 2023). Currently, most available therapies against *Leishmania* focus on targeting the parasite rather than including host-directed immunotherapies. Immunotherapy could provide therapeutic benefits for disease control as has been seen for cancer or could be part of a combination regimen with a direct antileishmanial.

The β-carbolines alkaloid harmine is a multikinase inhibitor that has shown inhibitory effects on monoamine oxidase A and selected kinases, including different members of the dual-specificity tyrosine-regulated kinases with the highest affinity for DYRK1A and CLK1 and CLK4 (Ahmad et al., 2020; Tarpley et al., 2021). It has broad anticancer activities, and ACB1801, a synthetic derivative, was recently shown to improve MHC-I–dependent antigen presentation in poorly immunogenic cancer cells resistant to anti–PD-1 (Noman et al., 2022). In this study, we tested the impact of ACB1801 on the host immune response and pathology during cutaneous leishmaniasis. After infection with the multidrug-resistant *L major* Seidman (*Lm*Sd) strain (Neva et al., 1979), ACB1801 treatment significantly improved MHC-II and costimulatory molecule expression in *Leishmania*-infected antigen-presenting cells in vitro and in vivo. Furthermore, treatment with ACB1801, once a lesion was apparent, led to a reduced cutaneous lesion evolution with a lower parasite burden. We show that ACB1801-dependent immune response improvement correlates with an increase of TNF-α/IFN-γ double-producing $CD4^+$ T cells and reduced T-cell–derived IL-10, a process mediated by the downregulation of AhR signaling.

RESULTS

Microbicidal effect of β-carboline derivative compounds on *Leishmania* promastigotes

To analyze a potential direct effect of β-carboline derivative compounds on *Leishmania* parasites, promastigote's susceptibility to ACB1801 and ACB1804, 2 β-carboline derivatives, was assessed, testing different concentrations (0.2–150 μM) against 2 strains of *Leishmania major* causing cutaneous leishmaniasis, *L major* LV39 and *Lm*Sd, and 1 species causing visceral leishmaniasis, *L donovani*. Exposure to ACB1801 displayed a parasiticidal effect with a half-maximal inhibitory concentration between 5 and 14 μM and had better killing activity than exposure to ACB1804 for the 3 *Leishmania* spp tested. However, the values of miltefosine, a currently used drug, were significantly better, displaying values at a half-maximal inhibitory concentration <6 μM (Figure 1a and Supplementary Figure S1a). Bone marrow–derived macrophages (BMDMs) were then tested after exposure to different concentrations of the 3 indicated compounds to define their half-maximal cytotoxicity concentration for uninfected macrophages. All showed similar half-maximal cytotoxicity concentration values (Supplementary Figure S1b). On the basis of these results, the selectivity index was determined. A better selectivity index for ACB1801 than for ACB1804 was confirmed, with lower values than those observed in the presence of miltefosine (Figure 1 and Supplementary Figure S1c). ACB1801 was then selected for further experiments.

ACB1801 mildly impacts intracellular amastigotes burden in BMDMs

We then investigated the role of ACB1801 in internalized *Leishmania*. To this end, BMDMs were infected with fluorescent *Leishmania* parasites at a multiplicity of infection of 10 for 24 hours. The cells were then treated with ACB1801, miltefosine, or their vehicle. Nonexposed infected cells were used as controls. Forty-eight hours later, infection rate and number of amastigotes per infected macrophage were determined using high-content microscopy (Figure 1b and c). On the basis of these results, the half-maximal inhibitory concentration of macrophage amastigotes for 3 strains was calculated (between 11 and 16 μM).

Thus, ACB1801 showed a leishmanicidal effect on both promastigotes and intracellular amastigotes for the 3 *Leishmania* tested, with a selectivity index varying between 4.5 and 15. However, the parasiticidal effects were significantly lower than those observed for miltefosine (Figure 1d).

ACB1801 increases MHC-II and costimulatory molecule expression on *Leishmania*-infected dendritic cells

Given the previous report on the effect of ACB1801 on antigen presentation improvement (Noman et al., 2022) and the crucial role of dendritic cells (DCs) as antigen-presenting cells also observed in *Leishmania* infection, we investigated the impact of ACB1801 on DCs after infection. Bone marrow–derived DCs (BMDCs) were infected with *L major* LV39, *Lm*Sd, or *L donovani* and treated with ACB1801 or its vehicle 3 hours after infection. The surface expression of MHC-II and costimulatory molecules was analyzed by flow cytometry 24 hours after infection. Treatment with ACB1801 significantly increased the surface expression of MHC-II, CD86, and CD40 compared with that in nontreated infected DCs (Figure 2a and b). Concurrently, ACB1801 treatment of *Leishmania*-infected DCs significantly decreased the immune checkpoint molecule PD-L1, a well-known immunosuppressor (Figure 2a and b). *Leishmania* infection alone increased the expression of CD40 and CD86 but only modulated weakly MHC-II and PD-L1 surface expression on BMDCs (Supplementary Figure S2a). Together, these results support the significant role of ACB1801 in enhancing the antigen-presenting capacity of *Leishmania*-infected DCs while concomitantly dampening the immune checkpoint–mediated negative regulation of T-cell responses.

ACB1801 monotherapy controls lesion development and parasite load in vivo

To evaluate the therapeutic effect of ACB1801 on *Leishmania* pathology in vivo, mice were infected with *Lm*Sd, a *L major* strain that developed a nonhealing, progressive, and severe cutaneous pathology despite early and sustained T helper (Th) 1 response and minimal Th2 and Th17 response (Anderson et al., 2005).

C57BL/6 mice were infected intradermally with *Lm*Sd metacyclic promastigotes, and 12 days after infection, when the lesion was established, they received 3 mg/kg of ACB1801 or vehicle solvent intraperitoneally (i.p.) for 16 consecutive days (Figure 3a). Ten days after treatment, a tendency to a decreased lesion size was observed in mice receiving ACB1801 compared with that in control mice, which became statistically significant at the end of treatment (Figure 3b and c). The parasite burden in the infected ears was significantly reduced upon ACB1801 treatment, but no difference was observed in draining lymph nodes (dLNs) (Figure 3d). We then increased the treatment regimen,

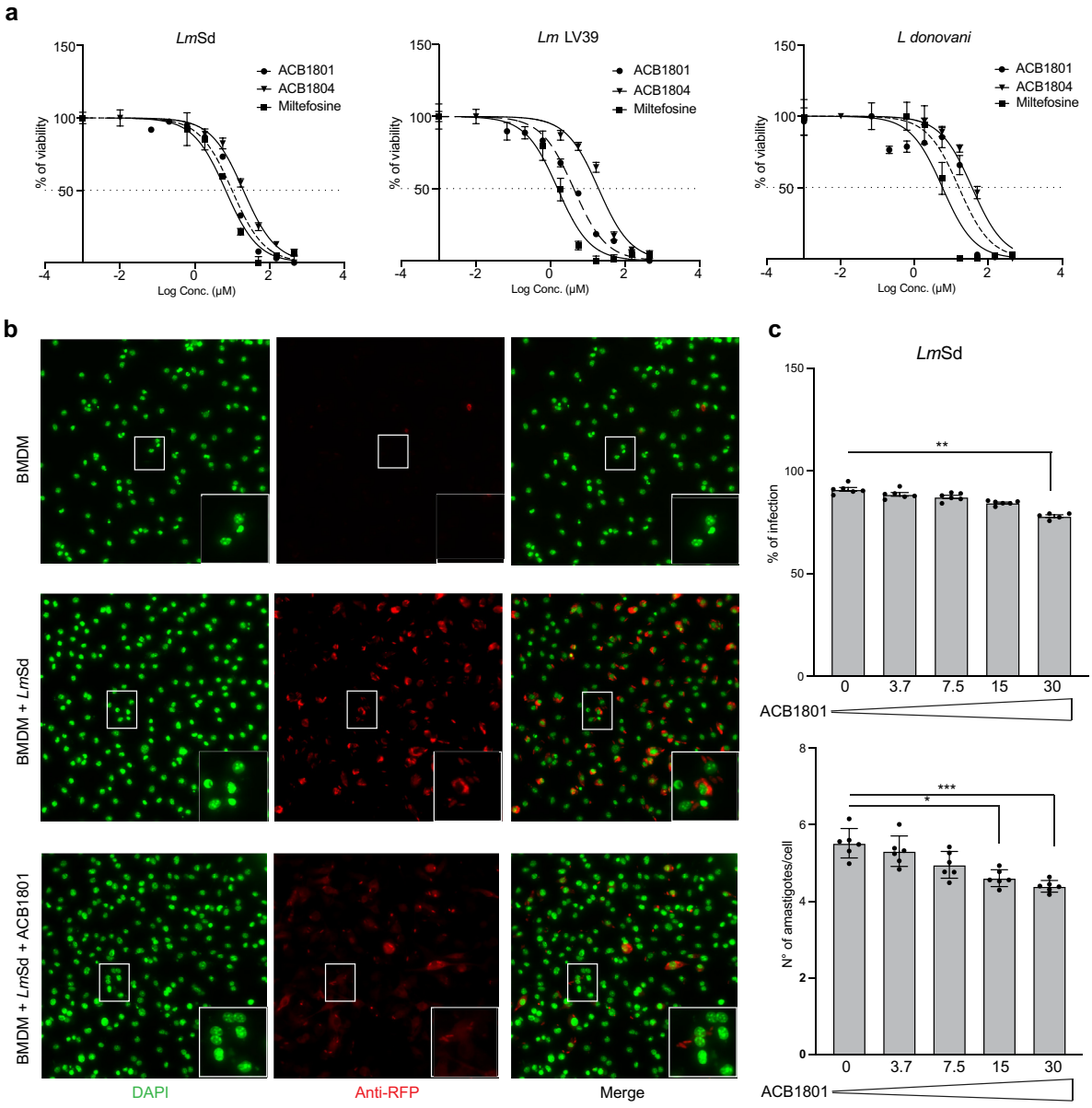

d

Cells	Parasite stage	ACB1801 CC50	ACB1801 IC50	ACB1801 SI	Miltefosine CC50	Miltefosine IC50	Miltefosine SI
BMDM	-	71.2			67		
Lm Sd	Promastigotes		7.9	9.2		4.5	14.8
	MΦ amastigotes		16.0	4.5		1.3	47.0
Lm LV39	Promastigotes		4.8	15		1.5	44.0
	MΦ amastigotes		11.6	6.5		2.5	26.6
L donovani	Promastigotes		14.0	5.3		5.7	11.7
	MΦ amastigotes		13.8	5.1		11.4	5.8

Figure 1. ACB1801 affects mildly intracellular amastigotes survival in BMDMs. (**a**) Metacyclic promastigotes were cultured for 48 h with ACB1801, ACB1804, and miltefosine at the indicated concentrations, and the IC50 was assessed. The figure is representative of 1 of 3 experiments (n = 3 per group). (**b**) BMDMs infected with *Lm*Sd at MOI of 10 were exposed to ACB1801 or diluent 24 h p.i. and analyzed 48 h later (72 h p.i.). Representative pictures of HCM showing uninfected macrophages (upper panel), *Lm*Sd-RFP–infected macrophages (middle panel), and *Lm*Sd-RFP–infected macrophages exposed to 30 μM of ACB1801 (lower panel). Nuclei are in green (DAPI), and fluorescent parasites are in red. (**c**) Frequency of infection and number of amastigotes per macrophage in the presence of the indicated doses of ACB1801. Data are represented as mean values ± SEM. The data are representative of 1 of 2 experiments (n = 8 per group). (**d**) Summary table giving the CC50, IC50, and SI for the tested *Leishmania*. LmLV39 denotes *Leishmania major LV39*. BMDM, bone marrow–derived

injecting ACB1801 twice a day (6 mg/kg 2 twice daily, i.p.), and compared the lesion size and parasite burden with those of mice treated for 16 days with vehicle and amphotericin B (10 mg/kg, twice weekly, i.p.), a potent conventional anti-leishmanial drug with serious side effects in human (Figure 3e). Both ACB1801 and amphotericin B treatment efficiently reduced lesion development compared with vehicle controls, with significant differences observed from 10 days after treatment until the end. ACB1801 efficiency was comparable with that of amphotericin B (Figure 3f–g). The parasite load in the infected ears of ACB1801- and amphotericin B–treated mice was significantly lower than that of control mice (Figure 3h).

These results indicate that ACB1801 treatment efficiently controls lesion development and parasite load after *Lm*Sd infection in vivo. Furthermore, considering the significant impact on DC activation observed in vitro and the mild parasiticidal effect of this compound, our data suggest an important role of ACB1801 in redirecting the immune response to infection.

ACB1801-treated dLNs reveal an enriched transcriptomic signature for IFN-γ and TNF-α

To unravel the mechanisms responsible for ACB1801-mediated effects on the immune response to *Lm*Sd infection in vivo, we performed RNA-sequencing analysis of dLNs isolated from *Lm*Sd-infected C57BL/6 mice treated with 6 mg/kg of ACB1801 twice daily (group 1) or vehicle (group 2) i.p. 10 days after treatment, when a significant effect of the treatment on lesion size was first observed (Figure 3f). The contralateral dLNs of the same mice were used as noninfected controls (groups 3 and 4) (Figure 4a). Altogether, 4 biological replicates per condition were sequenced.

Principal component analysis suggested that the 4 groups of samples are distinct, with *Lm*Sd infection accounting for over 50% variations (principal control 1 in Figure 4b). We focused on the infected samples to investigate the transcriptomic alterations induced by ACB1801 treatment upon *Lm*Sd infection. Sample LN2 was identified as an outlier owing to its distinct clustering pattern compared with the other samples within the same group and thus was removed for further analysis. Gene set enrichment analysis revealed that IFN-γ response and TNF-α signaling through NF-κb are among the top enriched Hallmark signatures (Figure 4c and d), with significantly positive correlations (Figure 4e). In line with our previously described in vitro data (Figure 2), ACB1801-induced gene expression also positively correlated to MHC-II antigen presentation signature (Figure 4e).

Taken together, the transcriptomic profiling supports our in vitro analysis and further highlights the potential roles of TNF-α– and IFN-γ–signaling pathways downstream of ACB1801 treatment.

ACB1801 reduces the frequency of $CD4^+IFN\text{-}\gamma^+$ $IL\text{-}10^+$ T cells and enhances that of proinflammatory macrophages

To validate the transcriptomics data at the protein level, the innate and adaptive immune responses in the dLNs and infected ears were analyzed following the same protocol, where mice were sacrificed 10 days after treatment. Flow cytometry analysis showed a 1.5-fold increase in the frequency of $CD4^+IFN\text{-}\gamma^+$ cells producing TNF-α in ACB1801-treated mice both in the dLNs (Figure 5a and Supplementary Figure S3a) and at the site of infection (Figure 5b). We confirmed a higher TNF-α production by dLNs cells after *Lm*Sd restimulation in vitro, as analyzed by ELISA (Supplementary Figure S3b). Double producer T cells have been shown to provide optimal effector function and protection against *L major* (Darrah et al., 2007). In addition, a subset of Th1 cells producing IFN-γ and IL-10 simultaneously was reported to contribute to the nonhealing phenotype observed in *Lm*Sd-infected C57BL/6 mice (Anderson et al., 2005). In this study, we show that upon β-carboline derivative treatment, the frequency of these $CD4^+IFN\text{-}\gamma^+IL\text{-}10^+$ double producers was significantly reduced, and a lower frequency of $CD4^+IL\text{-}10^+FoxP3^-$ cells, which are the main source of IL-10 production (Anderson et al., 2007), was observed (Figure 5a and b).

TNF-α produced by T cells induces a proinflammatory phenotype in macrophages and DCs (Schleicher et al., 2016). The macrophage and DC phenotypes of ear cells isolated from uninfected mice or infected mice treated or not with ACB1801 were analyzed by flow cytometry. Enhanced expression of MHC-II and CD86 was observed upon infection. Moreover, a significantly higher expression of these molecules was observed in ACB1801-treated mice than in vehicle-treated mice, suggesting improved antigen presentation and recognition (Figure 5c). Concurrently, they displayed a more proinflammatory and parasite-killing phenotype with higher expression of iNOS and TNF-α and moderately less arginase expression (Figure 5d).

Collectively, these results suggest that ACB1801 treatment decreases lesion development by shifting the balance toward a more antileishmanial healing phenotype with more $IFN\text{-}\gamma^+TNF\text{-}\alpha^+$-producing T cells, which affects the macrophage phenotype, and less IL-10 production.

AhR signaling is involved in ACB1801 mechanism of action

β-Carbolines, including harmine, can downregulate AhR signaling (El Gendy and El-Kadi, 2013). The immunomodulatory role of AhR was previously reported in inflammatory response by promoting IL-10 production and regulatory T cells (Apetoh et al., 2010; Mondanelli et al., 2019). We therefore checked the mRNA expression level of the main target genes of AhR in our RNA-sequencing datasets. We found in ACB1801-treated dLNs a significant downregulation of *Cyp1b1*, a well-established target gene for AhR activation. Further analysis also confirmed the downregulation of *MaoA*, *Maob*, and *Il4i1* genes in ACB1801-treated dLNs (Figure 6a). MAOA and MAOB are both regulated by AhR, and the former is an enzymatic target of harmine (Herraiz, 2007; Myburg et al., 2022). *Il4i1* is an immunosuppressive regulator of immune synapses and T-cell responses that is both a target gene and an indirect activator of AhR mediated through the generation of indole metabolites and kynurenic acid (Sadik et al., 2020). Given the clear role of AhR and indoleamine 2,3-

macrophage; CC50, half-maximal cytotoxicity concentration; Conc., concentration; h, hour; HCM, high content microscopy; IC50, half-maximal inhibitory concentration; LmSd, *Leishmania major* Seidman; MOI, multiplicity of infection; p.i., postinfection; SI, selectivity index.

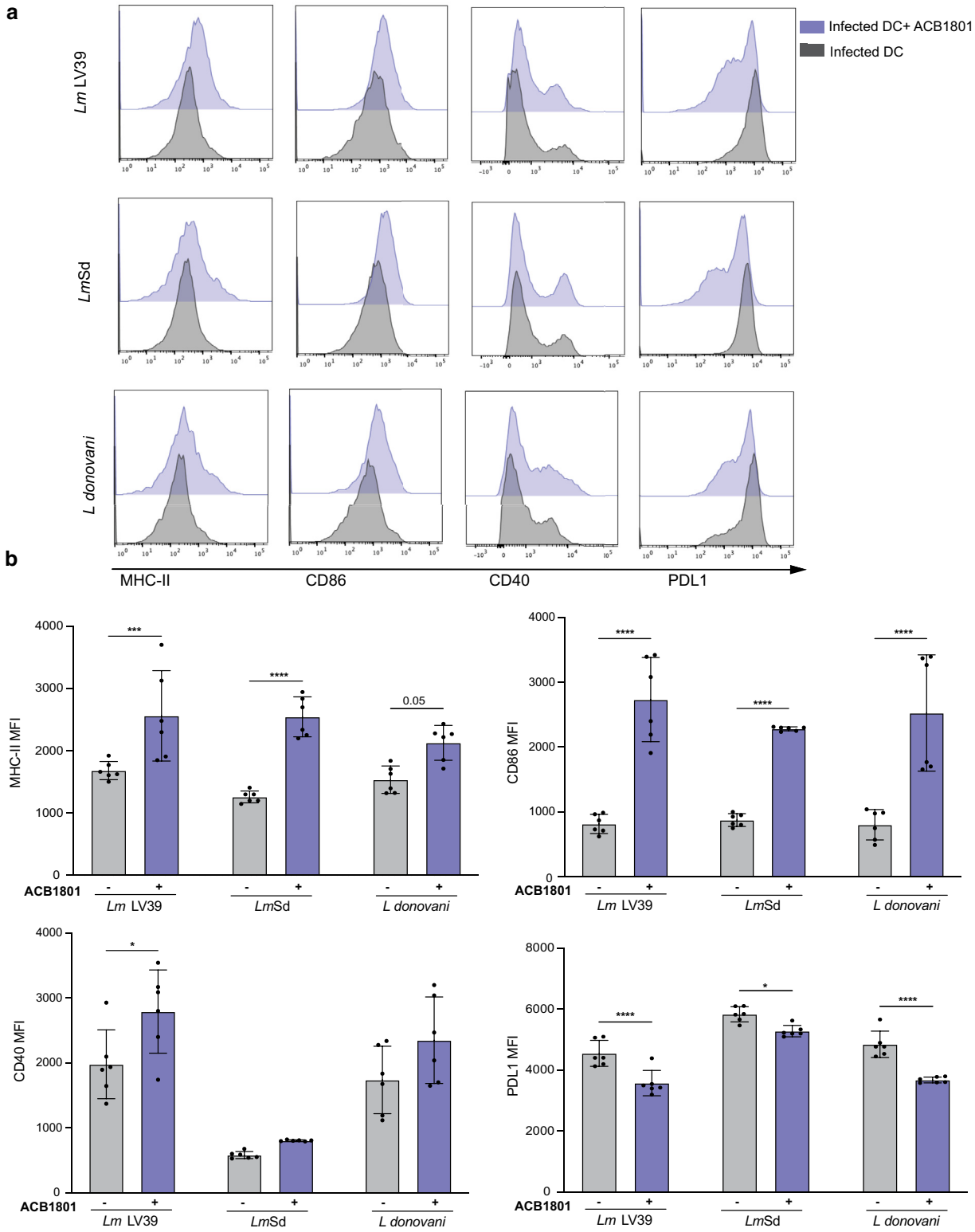

Figure 2. ACB1801 increases the expression of costimulatory molecules on dendritic cells. (a, b) A total of 4 × 10^5 BMDCs were infected with *Lm*Sd, *L major* LV39, and *L donovani* metacyclic promastigotes at a MOI of 10. After 3 h of infection, ACB1801 was added at 30 μM, and the expression of costimulatory molecules was analyzed by flow cytometry 24 h p.i. (**a**) Representative histograms showing the expression of the indicated costimulatory molecules in *Lm*Sd-infected DC (gray) and infected and ACB1801-treated DCs (purple). (**b**) The MFI of MHC-II, CD86, CD40, and PD-L1 on DC in the presence or absence of ACB1801 is shown. Data are a pool of 2 independent experiments (technical replicates = 3). Data are presented as mean values ± SEM. BMDC, bone marrow–derived dendritic cell; DC, dendritic cell; h, hour; LmSd, *Leishmania major* Seidman; MFI, mean fluorescence intensity; MHC-II, major histocompatibility complex class II; MOI, multiplicity of infection; p.i., postinfection.

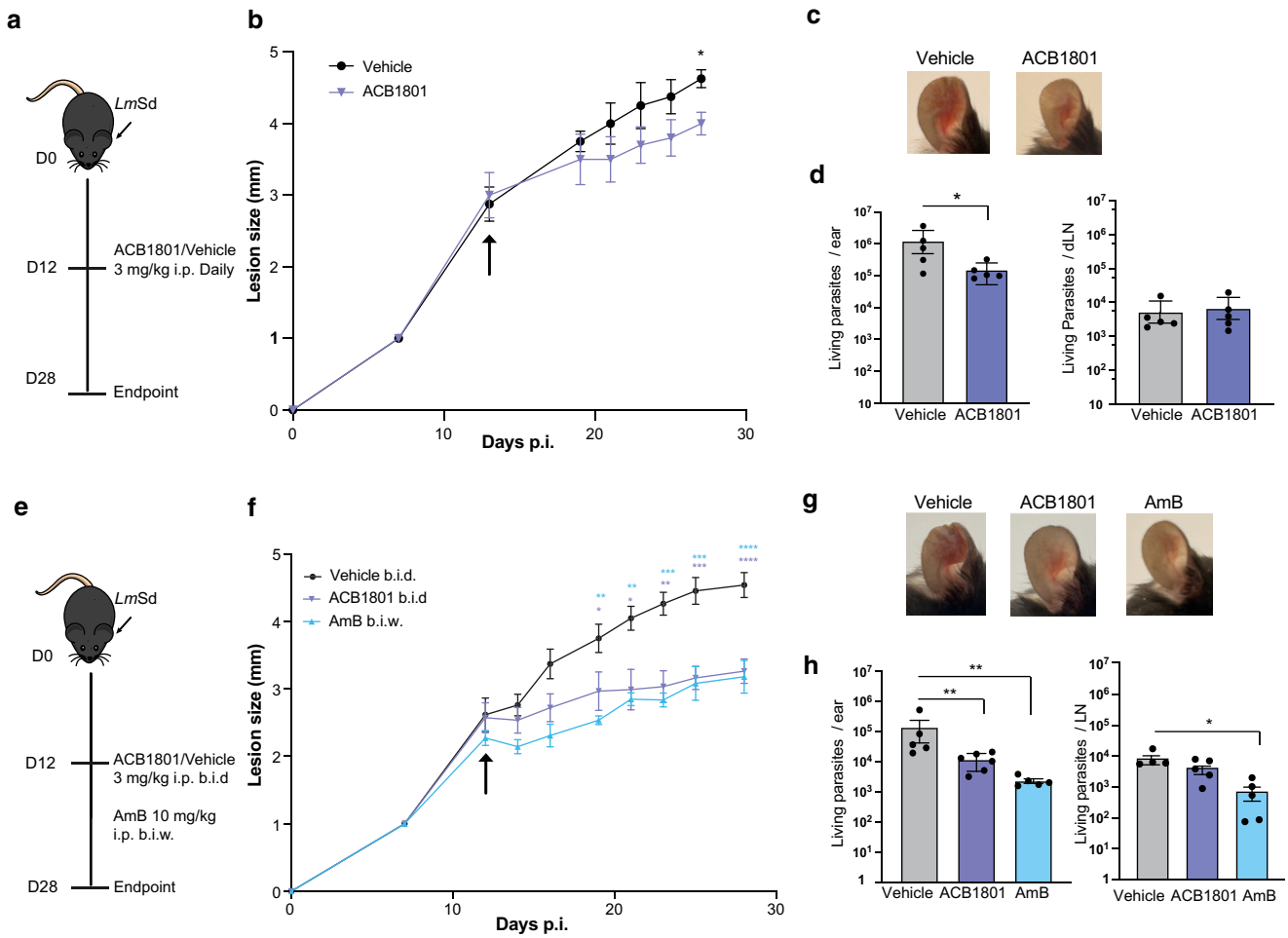

Figure 3. Injection of ACB1801 reduces significantly lesion development and parasite load. **(a)** Schematic experimental design: C57BL/6 mice were infected i.d. with 2 × 10^5 metacyclic *Lm*Sd and 12 days p.i. When the lesion was established, mice received 3 mg/kg daily of ACB1801 or vehicle i.p. **(b)** Lesion size was measured up to 28 days p.i. The arrow indicates the onset of drug treatment. (**c**) Representative pictures of the infected ear at the end of treatment. (**d**) Parasite load at the site of infection and dLNs 28 days after infection, analyzed by LDA. **(e)** Schematic experimental design: 6 mg/kg ACB1801 b.i.d. or AmB b.i.w. for 16 days. **(f)** Lesion size was measured up to 28 days p.i. **(g)** Representative pictures of the infected ear. **(h)** Parasite load at the site of infection and dLN 28 days p.i. Data are the mean ± SEM, representative of 2 independent experiments (n = 5 per experiment). D0, D12, and D28 denote day 0, day 12, and day 28, respectively. AmB, amphotericin B; b.i.d., twice daily; b.d.w., twice weekly; dLN, draining lymph node; i.d., intradermally; LDA, limiting dilution assay; LmSd, *Leishmania major* Seidman; p.i., postinfection.

dioxygenase (IDO) in immune responses, we focused on the effects of AhR and IDO at the protein level in vivo. The expression of AhR and IDO1 on dLN $CD4^+$ T cells was similar between uninfected and infected but significantly decreased in the presence of ACB1801 (Figure 6b, upper panel). In addition, very low expression of AhR and IDO1 was detected in uninfected DCs, but infection induced their expression, a process that was significantly decreased upon ACB1801 treatment (Figure 6b, lower panel).

To investigate the direct role of AhR inhibition on *Leishmania*-infected DC function, we exposed *LmSd*-infected BMDCs to antagonists for AhR (GNF351) or IDO (GNF-PF3777 and PF06840003). After 24 hours of infection, both AhR and IDO antagonists improved MHC-II and CD86 surface expression similar to what was observed after ACB1801 exposure (Figure 6c). To confirm the ACB1801 immunostimulatory role through AhR downregulation, we evaluated the expression level of MHC-II and CD86 on infected DCs in the presence of ACB1801 or a combination of ACB1801 and increasing doses of the AhR activator, FICZ. Upregulation of MHC-II and CD86 by ACB1801 was partially inhibited in the presence of FICZ, suggesting competition between the 2 drugs (Figure 6d and Supplementary Figure S4).

Taken together, these results suggest that the mechanism of action of ACB1801 in vivo could act through the down-regulation of AhR signaling.

DISCUSSION

The progression and maintenance of cutaneous diseases due to skin infections, such as those observed in cutaneous leishmaniasis, are partly dependent on the immune subversion of the host immune response by the parasites. Yet, most antileishmanial therapies target parasite survival within the host rather than the observed host immune impairment generated by infection. In this study, we report that ACB1801, a synthetic derivative of β-carboline harmine, has a major

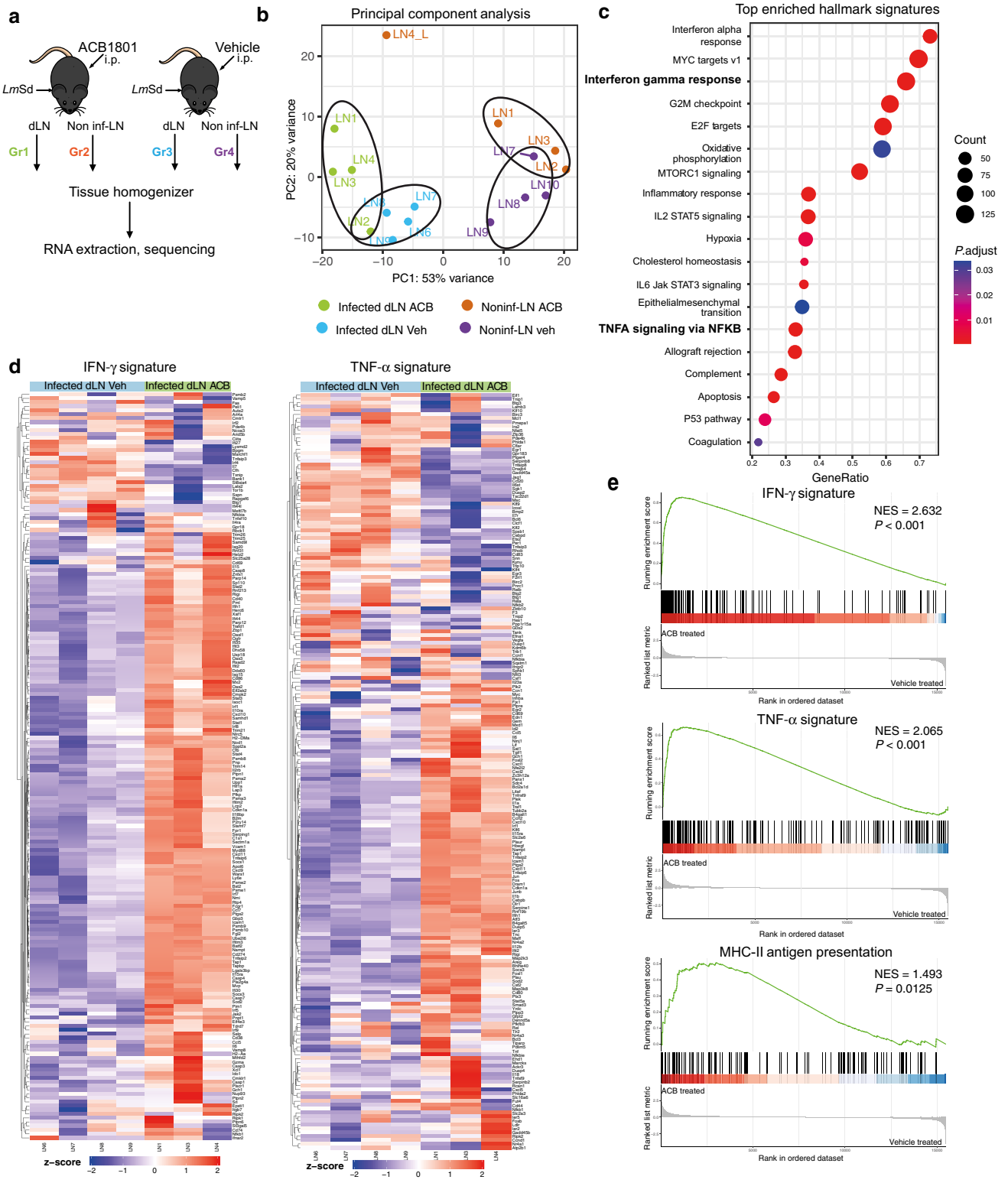

Figure 4. Transcriptomic profile of ACB-treated dLNs shows enrichment of IFN-γ and TNF-α signatures. **(a)** Illustrative scheme of experimental procedure to obtain samples for RNA sequencing. **(b)** Principal component analysis of the dLNs from mice treated with ACB1801 (group1) or vehicle (group2) and contralateral LNs as noninfected controls (groups 3 and 4). The distance along each axis represents the amount of variance in gene expression explained by the corresponding factor. (**c**) Scatter plot showing the significantly altered Hallmark signatures by GSEA. **(d)** Heatmap showing the expression of genes within the IFN-γ response and TNF-α signaling through NF-kB signature using the z-score of log_2-transformed normalized expression value. **(e)** Positive correlation enrichment of IFN-γ response, TNF-α signaling, and MHC-II antigen presentation signatures in the ACB-treated *Lm*Sd-infected LNs. Non inf-LN denotes noninfected lymph node, and veh denotes vehicle. ACB, β-carboline derivative; dLN, draining lymph node; GSEA, gene set enrichment analysis; i.p., intraperitoneal; LmSd, *Leishmania major* Seidman; LN, lymph node; MHC-II, major histocompatibility complex class II; NES, normalized enrichment score.

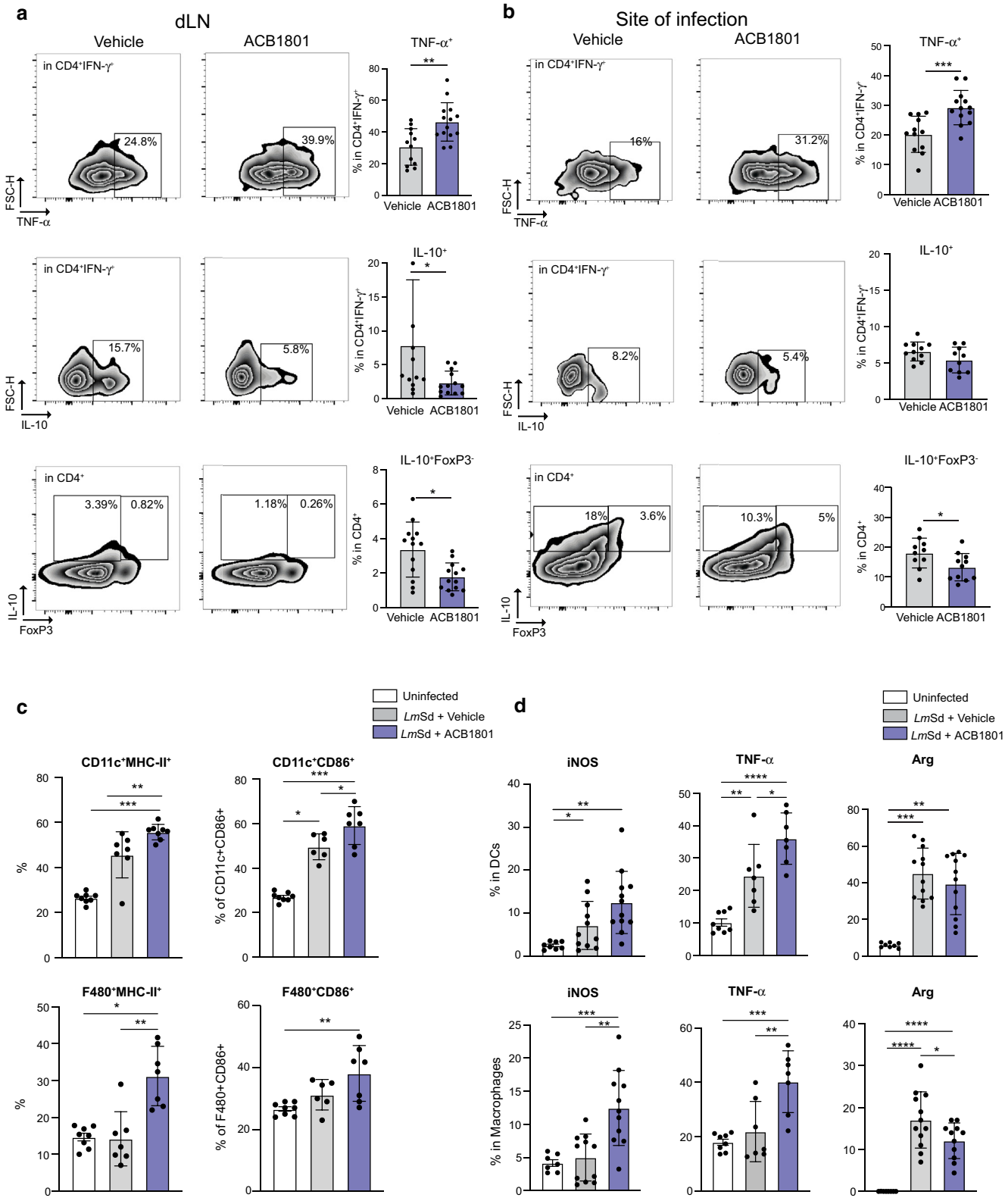

Figure 5. ACB1801 reduces the frequency of CD4$^+$IFN-γ$^+$ IL-10–producing T cells and enhances the polarization of proinflammatory macrophages. C57BL/6 mice were infected with 2 × 10^5 *Lm*Sd and 12 days p.i., treated for 10 days with ACB1801 or vehicle b.i.d. Mice were killed, and **(a)** dLNs and **(b)** ears were processed. Cells were stimulated in vitro with PMA and ionomycin for 4 h and analyzed by flow cytometry for intracellular cytokine production. Representative contour plots and histograms show the frequency of TNF-α and IL-10 in CD4$^+$IFN-γ$^+$ cells and FoxP3$^-$IL-10$^+$ in CD4$^+$ cells in ACB1801-treated versus vehicle mice. Data are a pool of 2 independent experiments (n = 12). **(c, d)** Expression of the indicated costimulatory molecules and proinflammatory markers on **(c)** DCs and **(d)** macrophages in uninfected, ACB-treated, or vehicle-treated infected ears. Data are presented as mean values ± SEM and are from 1 representative of 2 experiments (n = 8). ACB, β-carboline derivative; arg, arginine; b.i.d., twice daily; DC, dendritic cell; dLN, draining lymph node; FSC-H, forward scatter height; h, hour; iNOS, inducible nitric oxide synthase; LmSd, *Leishmania major* Seidman; p.i., postinfection; PMA, phorbol myristate acetate.

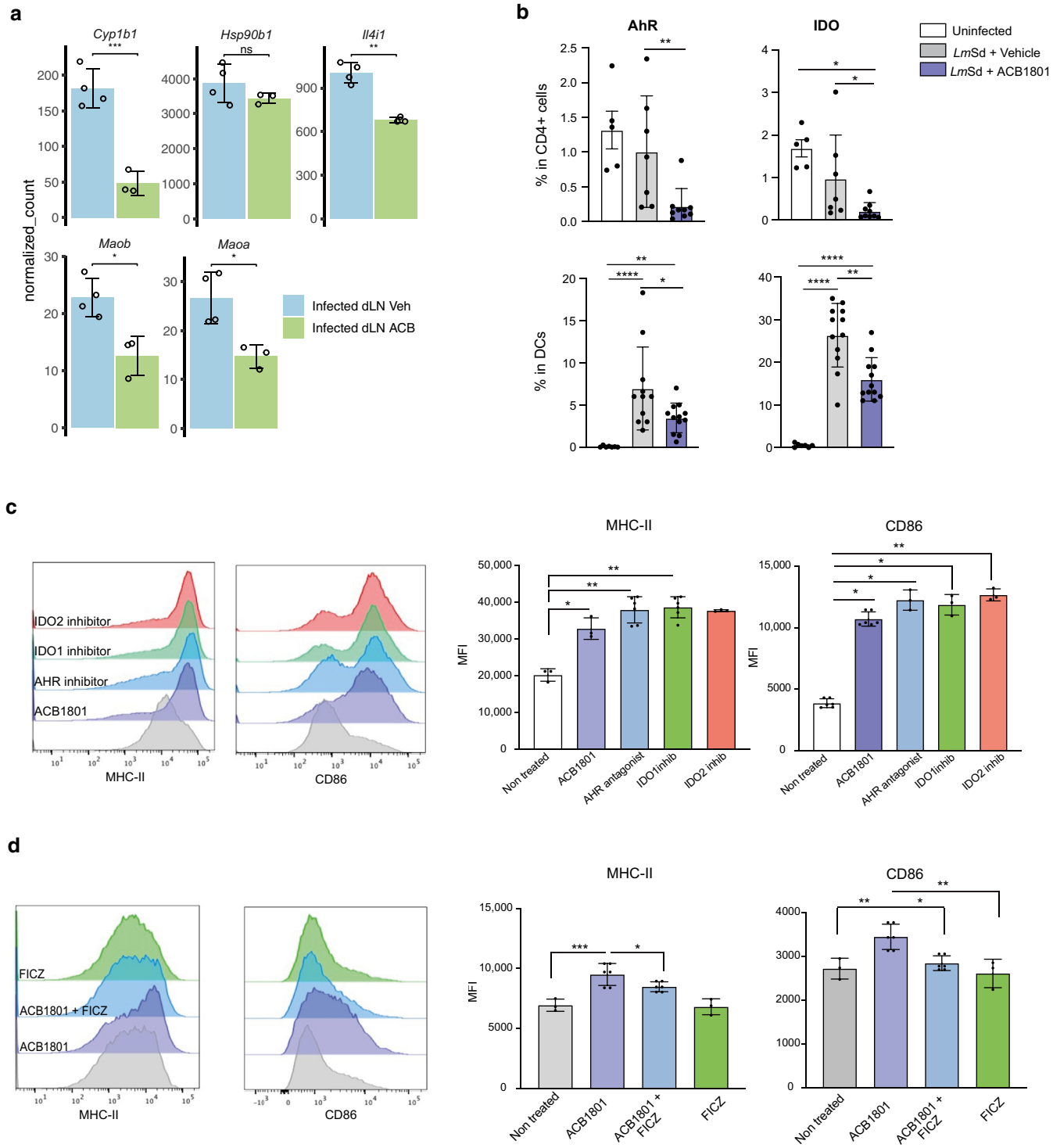

Figure 6. AhR signaling is downregulated in ACB1801-treated cells. **(a)** mRNA expression of *Cyp1b1*, *Hsp90b1*, *Il4i1*, *Maob*, and *Maoa* analyzed from RNAseq dataset. Each dot represents 1 biological replicate. Data presented as normalized expression values (mean ± SD). **(b)** Frequency of intracellular AhR and IDO expression in $CD4^+$ T cells and DCs in dLNs from *Lm*Sd-infected and -uninfected mice treated for 10 days with ACB1801 (6 mg/kg) or vehicle b.i.d. The data are from 1 representative of 2 experiments (n = 8 for infected, n = 5 for uninfected). **(c, d)** BMDCs were infected with *LmSd* at MOI of 10; 3 h later, cells were exposed to **(c)** 30 μM ACB1801, 1 μM GNF351, 0.5 μM GNF-PF3777, or 3 μM PF06840003 for 24 h after infection. **(d)** A total of 30 μM ACB1801 in the presence or absence of AhR activator FICZ. Representative histogram showing MHC-II and CD86 expression with the corresponding MFI. The data are a pool of 2 independent experiments (technical n = 3). AhR, aryl hydrocarbon receptor; b.i.d., twice daily; BMDC, bone marrow–derived dendritic cell; DC, dendritic cell; IDO, indoleamine 2,3-dioxygenase; h, hour; LmSd, *Leishmania major* Seidman; MFI, mean fluorescence intensity; MHC-II, major histocompatibility complex class II; MOI, multiplicity of infection; RNAseq, RNA sequencing.

impact on host immune response and the pathology during cutaneous leishmaniasis.

Intracellular protozoan parasites, including *Leishmania* or *Trypanosoma*, disturb T-cell activation by impairing the MHC-II and costimulatory molecules expression on DCs (Chakraborty et al., 2005; Sibley, 2011; von Stebut and Tenzer, 2018). ACB1801 has been shown recently to improve immune response in poorly immunogenic B16-F10 melanoma mouse tumors by increasing their MHC-I expression (Noman et al., 2022). We first showed that ACB1801 had a mild parasiticidal effect on free and macrophage-internalized parasites. The major outcome of exposure to the drug was increased activation of *Leishmania*-exposed DCs, including higher expression of the CD40 and CD86 costimulatory molecules and MHC-II, all essential in antigen presentation to elicit antileishmanial adaptive response (de Freitas e Silva and von Stebut, 2021).

Host immune responses against *Leishmania* depend in part on IFN-γ–producing $CD4^+$ Th1 cells, which activate macrophage leishmanicidal activity. The immunologic mechanisms underlying nonhealing forms of leishmaniasis in mice were initially studied in the context of Th2-polarized response in BALB/C mice, with high levels of IL-4 driving permissive M2-like macrophages. However, Th dichotomy does not always correlate with resistance or susceptibility to infection (Tacchini-Cottier et al., 2012), and the processes involved in nonhealing forms of cutaneous leishmaniasis observed in humans were shown to include an enriched environment of proinflammatory cytokines, and high levels of IL-10 can be observed (Louzir et al., 1998; Melby et al., 1994; Nylén and Sacks, 2007).

Infection with *Lm*Sd results in the development of nonhealing exacerbated lesions in C57BL/6 mice in the presence of a strong $CD4^+$Th1, a process correlated with elevated levels of $CD4^+IL10^+FoxP3^-$ cells (Anderson et al., 2007, 2005). Our in vivo data show an important impact on pathology and parasite burden after ACB1801 treatment. RNA-sequencing data from infected and ACB1801-treated dLNs revealed enrichment of TNF-α and IFN-γ pathways. Optimal Th1 effector function relies not only on IFN-γ production but also on TNF-α production as shown for *Leishmania* (Darrah et al., 2007). The increased frequency of IFN-γ and TNF-α producing CD4 T cells in parallel to decreased T-cell–derived IL-10 production was confirmed at the protein level, which shifts the balance toward a more protective response.

IFN-γ and TNF-α activate macrophages and DCs by switching arginine metabolism toward the production of nitric oxide through iNOS (Gogoi et al., 2016; Schleicher et al., 2016). In *Lm*Sd ACB1801–treated mice, we also observed an increased frequency of iNOS expression in both macrophages and DCs at the site of infection, which could be responsible for the decreased parasite burden. Arginine and tryptophan metabolism are linked through the activities of ARG1 and IDO1 (Crowther and Qualls, 2021; Mondanelli et al., 2019), and both can affect macrophage polarization. Harmine was previously shown to inhibit the induction of CYP1A1, a carcinogen activator enzyme, by inhibiting AhR signaling (El Gendy and El-Kadi, 2013). Only a few studies investigated the role of AhR in cutaneous leishmaniasis, reporting mostly increased inflammatory cytokines production (Climaco-Arvizu et al., 2016; Münck et al., 2019; Oljuskin et al., 2023). In addition, several studies demonstrate nongenomic and post-transcriptional roles for AhR (Großkopf et al., 2021; Luecke-Johansson et al., 2017), and nongenomic AhR signaling was shown to play immunomodulatory roles through signal transducer and activator of transcription 3 phosphorylation and IL-10 production (Zhu et al., 2018).

To investigate the mechanism behind the observed immunomodulatory effect of ACB1801 treatment, we checked our RNA-sequencing data AhR signaling partners expression. Our transcriptomics data did not correlate significantly with previously published AhR signatures (Castellano et al., 2021; Franchini et al., 2019; Sadik et al., 2020). Yet, prototypical selected AhR target genes were downregulated during ACB1801 treatment, notably, *Cyp1a1*, *Cyp1b1*, *IL4il*, *Maoa*, and *Maob*. In correlation with these data, our in vivo results revealed a decrease in AhR frequency in both $CD4^+$ T cells and DCs in ACB1801-treated dLNs. To establish a direct correlation between AhR and ACB1801, *Leishmania*-infected BMDCs were treated with ACB1801 in the presence or absence of AhR activator. Competition between these 2 drugs was demonstrated.

In summary, our data reveal, to our knowledge, a potential previously unreported drug against nonhealing form of cutaneous leishmaniasis. ACB1801 used as monotherapy had a significant impact on the pathology by promoting a protective immune response and dampening immunosuppressive IL-10–producing $CD4^+$ T cells. A potential use of this drug as monotherapy or in combination with conventional therapies could be envisaged to decrease current regimen or duration of treatment.

MATERIALS AND METHODS

Mice and ethics

C57BL/6 mice (Charles River Laboratories) were bred under specific pathogen-free conditions at the animal facility of the University of Lausanne (Epalinges, Switzerland). Mice aged 6–8 weeks were used for the experiments. Animal experimentation protocols were approved by the veterinary office of the Canton of Vaud (Authorization VD3616A to FTC). They were performed per cantonal and federal laws and the ethics principles of the Declaration of Basel.

Parasite culture and infections

*Lm*Sd (MHOM/SN/74/S.D.), *L major* LV39 (MRHO/Sv/59/P), and *L donovani* (LV9) and parasites expressing RFPs (*L major* LV39 mcherry [Ronet et al., 2019] and *L major* Sd-RFP [Peters et al., 2008]) were cultured in rabbit agar blood in 10 ml of supplemented M199 10% heat-inactivated fetal bovine serum, 4% 4-(2-hydroxyethyl)piperazine-1-ethane-sulfonic acid (Amimed), and 100 U/ml penicillin and 100 μg/ml streptomycin (Invitrogen) at 26 °C. Fluorescent were also used. Metacyclic promastigotes were isolated by density gradient as previously described (Späth GF, Beverley, 2001).

BMDM and BMDC generation

Isolated femurs and tibia were flushed, and cells were cultured with complete RPMI as with 20 ng/ml GM-CSF (12343127, ImmunoTools) for BMDC differentiation and 25 ng/ml macrophage colony-stimulating factor (12343117, ImmunoTools) for BMDMs for 7 days.

Drugs and treatments

For in vivo treatments, ACB1801 and ACB1804 were prepared by AC Bioscience SA. β-Carboline derivative was diluted in PBS (10% DMSO), and mice were injected with 100 µl ACB1801 3 mg/kg in a single daily dose (3 mg/kg) or twice per day (6 mg daily/kg) i.p. Miltefosine (hexadecyl phosphocholine [58066-85-6]) from Cayman Chemicals and amphotericin B (HY-V0221) from MedChemExpress were used as reference drugs. For in vitro experiments, cells were cultured in RPMI 0.1% DMSO including or not (vehicle) ACB1801 at 30 µM.

Half-maximal effective concentration determination using high content microscopy

BMDMs were infected with *L major* mCherry or *L major* Sd-RFP, and the half-maximal effective concentration was measured by high-content microscopy as detailed in Supplementary Materials and Methods. The image acquisition was performed using the ImageXpress Micro C (confocal) high-content imaging system (Eren et al., 2018), which takes 25 images for each replicate. The fluorescence background observed in uninfected macrophages (3−5%) was subtracted for parasite counting.

Mice infection and treatment protocol in vivo

C57BL/6 mice were needle inoculated with 2×10^5 *Lm*Sd metacyclic promastigotes into the ear dermis (intradermally). The lesion size was analyzed as previously described (Schuster et al., 2014). The treatments were started once the lesion reached a score of 2 (visible lesion) on day 12 after infection. Ears and lymph nodes were recovered and processed into a single-cell suspension as previously described (Passelli et al., 2022).

RNA sequencing

dLNs and contralateral lymph nodes were collected in RLT plus buffer and homogenized using tissue lyzer. mRNA was extracted using Qiagen RNAeasy mini kit. cDNA libraries were prepared, and RNA sequencing was performed as detailed in the Supplementary Materials and Methods.

Flow cytometry analysis

Stained dLNs and ear cells were isolated, stained, and analyzed using LSR-Fortessa (BD Bioscience) as previously described (Passelli et al., 2022) and analyzed with FlowJo software (version 10). The antibodies used are provided in the Supplementary Materials and Methods.

Limiting dilution assay

To estimate the number of living parasites, single-cell suspensions from infected mice were serially diluted in supplemented M199 media. The number of parasites was determined using the ESTIMFRE software as previously described (Titus et al., 1985).

Statistics

For comparison between 2 sample groups with a normal distribution, statistics were assessed by a nonparametric unpaired *t*-test (Mann−Whitney *U* test). Comparisons of more than 2 groups were made by 1-way ANOVA and Bonferroni posthoc test. $*P < .05$, $**P < .005$, $***P < .0002$, and $****P < .0001$; ns denotes no significance.

Data availability statement

The RNA-sequencing data produced in this study have been deposited in the Gene Expression Omnibus with access code GSE236962.

ORCIDs

Sanam Peyvandi: http://orcid.org/0000-0002-3231-1116
Qiang Lan: http://orcid.org/0000-0002-7765-6767
Antoine Chabloz: http://orcid.org/0000-0001-8229-6877
Florence Prevel: http://orcid.org/0009-0007-4839-4773
Yazmin Hauyon La Torre: http://orcid.org/0009-0001-3692-7540
Annette Ives: http://orcid.org/0000-0002-7407-960X
Fabienne Tacchini-Cottier: http://orcid.org/0000-0003-3561-0207

CONFLICT OF INTEREST

AC and AI are employees at AC Bioscience. The research was undertaken in the absence of any commercial relationship that could be viewed as a conflict of interest. The remaining authors state no conflict of interest.

ACKNOWLEDGMENTS

We thank all group members for discussions, the members of the UNIL flow cytometry platform for excellent technical assistance, and Dimitry Moreau from the University of Geneva for assistance in the high-content microscopy. We also thank David Sacks for giving us *Leishmania major* Seidman and Christian Auclair, AC Biosciences for stimulating discussions. This work was funded by the Innosuisse-Swiss Innovation Agency, project 43914.1 IP-Life Sciences to FTC, and partially by related funding by AC BioScience SA.

AUTHOR CONTRIBUTIONS

Conceptualization: FT-C, AI; Formal Analysis: SP, QL, AI; Investigation: SP, AI, FT-C; Supervision: FT-C, AI, SP; Writing - Original Draft Preparation: SP, FT-C, AI; Writing - Review and editing: SP, QL, AC, FP, YHLT, AI, FT-C

SUPPLEMENTARY MATERIAL

Supplementary material is linked to the online version of the paper at www.jidonline.org, and at https://doi.org/10.1016/j.jid.2023.09.280.

REFERENCES

Ahmad I, Fakhri S, Khan H, Jeandet P, Aschner M, Yu ZL. Targeting cell cycle by β-carboline alkaloids in vitro: novel therapeutic prospects for the treatment of cancer. Chem Biol Interact 2020;330:109229.

Alpern D, Gardeux V, Russeil J, Mangeat B, Meireles-Filho ACA, Breysse R, et al. BRB-seq: ultra-affordable high-throughput transcriptomics enabled by bulk RNA barcoding and sequencing. Genome Biol 2019;20:71.

Anderson CF, Mendez S, Sacks DL. Nonhealing infection despite Th1 polarization produced by a strain of *Leishmania major* in C57BL/6 mice. J Immunol 2005;174:2934−41.

Anderson CF, Oukka M, Kuchroo VJ, Sacks D. CD4(+)CD25(−)Foxp3(−) Th1 cells are the source of IL-10−mediated immune suppression in chronic cutaneous leishmaniasis. J Exp Med 2007;204:285−97.

Apetoh L, Quintana FJ, Pot C, Joller N, Xiao S, Kumar D, et al. The aryl hydrocarbon receptor interacts with c-Maf to promote the differentiation of type 1 regulatory T cells induced by IL-27. Nat Immunol 2010;11:854−61.

Bogdan C. Macrophages as host, effector and immunoregulatory cells in leishmaniasis: impact of tissue micro-environment and metabolism. Cytokine X 2020;2:100041.

Bunn PT, Montes de Oca M, de Labastida Rivera F, Kumar R, Ng SS, Edwards CL, et al. Distinct roles for CD4+ Foxp3+ regulatory T cells and IL-10-mediated immunoregulatory mechanisms during experimental visceral leishmaniasis caused by Leishmania donovani. J Immunol 2018;201:3362−72.

Caldas A, Favali C, Aquino D, Vinhas V, van Weyenbergh J, Brodskyn C, et al. Balance of IL-10 and interferon-γ plasma levels in human visceral leishmaniasis: implications in the pathogenesis. BMC Infect Dis 2005;5:113.

Castellano F, Prevost-Blondel A, Cohen JL, Molinier-Frenkel V. What role for AHR activation in IL4I1-mediated immunosuppression. Oncoimmunology 2021;10:1924500.

Chakraborty D, Banerjee S, Sen A, Banerjee KK, Das P, Roy S. Leishmania donovani affects antigen presentation of macrophage by disrupting lipid rafts. J Immunol 2005;175:3214−24.

Climaco-Arvizu S, Domínguez-Acosta O, Cabañas-Cortés MA, Rodríguez-Sosa M, Gonzalez FJ, Vega L, et al. Aryl hydrocarbon receptor influences nitric oxide and arginine production and alters M1/M2 macrophage polarization. Life Sci 2016;155:76−84.

Costa-Madeira JC, Trindade GB, Almeida PHP, Silva JS, Carregaro V. T lymphocyte exhaustion during human and experimental visceral leishmaniasis. Front Immunol 2022;13:835711.

Crowther RR, Qualls JE. Metabolic regulation of immune responses to Mycobacterium tuberculosis: a spotlight on L-arginine and L-tryptophan metabolism. Front Immunol 2021;11:628432.

Darrah PA, Patel DT, De Luca PM, Lindsay RWB, Davey DF, Flynn BJ, et al. Multifunctional TH1 cells define a correlate of vaccine-mediated protection against *Leishmania major*. Nat Med 2007;13:843–50.

de Freitas e Silva R, von Stebut E. Unraveling the role of immune checkpoints in leishmaniasis. Front Immunol 2021;12:620144.

Durinck S, Moreau Y, Kasprzyk A, Davis S, De Moor B, Brazma A, et al. BioMart and Bioconductor: a powerful link between biological databases and microarray data analysis. Bioinformatics 2005;21:3439–40.

Durinck S, Spellman PT, Birney E, Huber W. Mapping identifiers for the integration of genomic datasets with the R/Bioconductor package biomaRt. Nat Protoc 2009;4:1184–91.

eBioMedicine. Leishmania: an urgent need for new treatments. EBioMedicine 2023;87:104440.

El Gendy MAM, El-Kadi AOS. Harmine and harmaline downregulate TCDD-induced Cyp1a1 in the livers and lungs of C57BL/6 mice. Biomed Res Int 2013;2013:258095.

Elizondo G, Rodríguez-Sosa M, Estrada-Muñiz E, Gonzalez FJ, Vega L. Deletion of the aryl hydrocarbon receptor enhances the inflammatory response to *Leishmania major* infection. Int J Biol Sci 2011;7:1220–9.

Eren RO, Kopelyanskiy D, Moreau D, Chapalay JB, Chambon M, Turcatti G, et al. Development of a semi-automated image-based high-throughput drug screening system. Front Biosci (Elite Ed) 2018;10:242–53.

Franchini AM, Myers JR, Jin GB, Shepherd DM, Lawrence BP. Genome-wide transcriptional analysis reveals novel AhR targets that regulate dendritic cell function during influenza A virus infection. Immunohorizons 2019;3:219–35.

Gogoi M, Datey A, Wilson KT, Chakravortty D. Dual role of arginine metabolism in establishing pathogenesis. Curr Opin Microbiol 2016;29:43–8.

Großkopf H, Walter K, Karkossa I, von Bergen M, Schubert K. Non-genomic AhR-signaling modulates the immune response in endotoxin-activated macrophages after activation by the environmental stressor BaP. Front Immunol 2021;12:620270.

Gu Z, Eils R, Schlesner M. Complex heatmaps reveal patterns and correlations in multidimensional genomic data. Bioinformatics 2016;32:2847–9.

Herraiz T. Identification and occurrence of β-carboline alkaloids in raisins and inhibition of monoamine oxidase (MAO). J Agric Food Chem 2007;55:8534–40.

Lee SH, Charmoy M, Romano A, Paun A, Chaves MM, Cope FO, et al. Mannose receptor high, M2 dermal macrophages mediate nonhealing *Leishmania major* infection in a Th1 immune environment. J Exp Med 2018;215:357–75.

Louzir H, Melby PC, Ben Salah A, Marrakchi H, Aoun K, Ben Ismail R, et al. Immunologic determinants of disease evolution in localized cutaneous leishmaniasis due to *Leishmania major*. J Infect Dis 1998;177:1687–95.

Love MI, Huber W, Anders S. Moderated estimation of fold change and dispersion for RNA-seq data with DESeq2. Genome Biol 2014;15:550.

Luecke-Johansson S, Gralla M, Rundqvist H, Ho JC, Johnson RS, Gradin K, et al. A molecular mechanism to switch the aryl hydrocarbon receptor from a transcription factor to an E3 ubiquitin ligase. Mol Cell Biol 2017;37:e00630–716.

Mann S, Frasca K, Scherrer S, Henao-Martínez AF, Newman S, Ramanan P, et al. A review of leishmaniasis: current knowledge and future directions. Curr Trop Med Rep 2021;8:121–32.

Martínez-Salazar B, Carregaro Pereira V, Hauyon-La-Torre Y, Khamesipour A, Tacchini-Cottier F. Evaluation of a new topical treatment for the control of cutaneous leishmaniasis. Microorganisms 2020;8:1803.

Melby PC, Andrade-Narvaez FJ, Darnell BJ, Valencia-Pacheco G, Tryon VV, Palomo-Cetina A. Increased expression of proinflammatory cytokines in chronic lesions of human cutaneous leishmaniasis. Infect Immun 1994;62:837–42.

Mondanelli G, Iacono A, Allegrucci M, Puccetti P, Grohmann U. Immunoregulatory interplay between arginine and tryptophan metabolism in health and disease. Front Immunol 2019;10:1565.

Münck NA, Roth J, Sunderkötter C, Ehrchen J. Aryl hydrocarbon receptor-signaling regulates early *Leishmania major*-induced cytokine expression. Front Immunol 2019;10:2442.

Myburg T, Petzer A, Petzer JP. The inhibition of monoamine oxidase by harmine derivatives. Results in Chemistry 2022;4:100607.

Neva FA, Wyler D, Nash T. Cutaneous leishmaniasis—a case with persistent organisms after treatment in presence of normal immune response. Am J Trop Med Hyg 1979;28:467–71.

Noman MZ, Bocci IA, Karam M, Moer KV, Bosseler M, Kumar A, et al. The β-carboline harmine improves the therapeutic benefit of anti-PD1 in melanoma by increasing the MHC-I-dependent antigen presentation. Front Immunol 2022;13:980704.

Nylén S, Sacks D. Interleukin-10 and the pathogenesis of human visceral leishmaniasis. Trends Immunol 2007;28:378–84.

Oljuskin T, Azodi N, Volpedo G, Bhattacharya P, Markle HL, Hamano S, et al. *Leishmania major* centrin knock-out parasites reprogram tryptophan metabolism to induce a pro-inflammatory response. iScience 2023;26:107593.

Passelli K, Prat-Luri B, Merlot M, Goris M, Mazzone M, Tacchini-Cottier F. The c-MET receptor tyrosine kinase contributes to neutrophil-driven pathology in cutaneous leishmaniasis. PLoS Pathog 2022;18:e1010247.

Peters NC, Egen JG, Secundino N, Debrabant A, Kimblin N, Kamhawi S, et al. In vivo imaging reveals an essential role for neutrophils in leishmaniasis transmitted by sand flies [published correction appears in Science 2008;322:1634]. Science 2008;321:970–4.

Ronet C, Passelli K, Charmoy M, Scarpellino L, Myburgh E, Hauyon La Torre Y, et al. TLR2 signaling in skin nonhematopoietic cells induces early neutrophil recruitment in response to *Leishmania major* infection. J Invest Dermatol 2019;139:1318–28.

Rothhammer V, Quintana FJ. The aryl hydrocarbon receptor: an environmental sensor integrating immune responses in health and disease. Nat Rev Immunol 2019;19:184–97.

Sadik A, Somarribas Patterson LF, Öztürk S, Mohapatra SR, Panitz V, Secker PF, et al. IL4I1 is a metabolic immune checkpoint that activates the AHR and promotes tumor progression. Cell 2020;182:1252–70.e34.

Schleicher U, Paduch K, Debus A, Obermeyer S, König T, Kling JC, et al. TNF-mediated restriction of arginase 1 expression in myeloid cells triggers Type 2 NO synthase activity at the site of infection. Cell Rep 2016;15:1062–75.

Schuster S, Hartley MA, Tacchini-Cottier F, Ronet C. A scoring method to standardize lesion monitoring following intra-dermal infection of Leishmania parasites in the murine ear. Front Cell Infect Microbiol 2014;4:67.

Sibley LD. Invasion and intracellular survival by protozoan parasites. Immunol Rev 2011;240:72–91.

Späth GF, Beverley SM. A lipophosphoglycan-independent method for isolation of infective Leishmania metacyclic promastigotes by density gradient centrifugation. Exp Parasitol 2001;99:97–103.

Subramanian A, Tamayo P, Mootha VK, Mukherjee S, Ebert BL, Gillette MA, et al. Gene set enrichment analysis: A knowledge-based approach for interpreting genome-wide expression profiles. Proc Natl Acad Sci 2005;102:15545–50.

Tacchini-Cottier F, Weinkopff T, Launois P. Does T helper differentiation correlate with resistance or susceptibility to infection with L. major? Some insights from the murine model. Front Immunol 2012;3:32.

Tarpley M, Oladapo HO, Strepay D, Caligan TB, Chdid L, Shehata H, et al. Identification of harmine and β-carboline analogs from a high-throughput screen of an approved drug collection; profiling as differential inhibitors of DYRK1A and monoamine oxidase A and for in vitro and in vivo anticancer studies. Eur J Pharm Sci 2021;162:105821.

Titus RG, Marchand M, Boon T, Louis JA. A limiting dilution assay for quantifying *Leishmania major* in tissues of infected mice. Parasite Immunol 1985;7:545–55.

von Stebut E, Tenzer S. Cutaneous leishmaniasis: distinct functions of dendritic cells and macrophages in the interaction of the host immune system with *Leishmania major*. Int J Med Microbiol 2018;308:206–14.

Yu G, Wang L-G, Han Y. He Q-Y. clusterProfiler: an R package for comparing biological themes among gene clusters. OMICS 2012;16:284–7.

Zhu J, Luo L, Tian L, Yin S, Ma X, Cheng S, et al. Aryl hydrocarbon receptor promotes IL-10 expression in inflammatory macrophages through Src-STAT3 signaling pathway. Front Immunol 2018;9:2033.

SUPPLEMENTARY MATERIALS AND METHODS

Parasite growth and half-maximal inhibitory concentration determination

The half-maximal inhibitory concentration (IC50) and half-maximal effective concentration (CC50) were determined as previously described (Martínez-Salazar et al., 2020). The IC50 is defined as the drug concentration causing 50% inhibition of proliferation compared with that of untreated parasites. A serial dilution of the drugs ranging from 0.2 to 150 μM was added subsequently. After 48 hours of incubation at 26 °C, Alamar blue was added to the samples at a 1× final concentration and incubated for 18 hours following the manufacturer's instructions. Then, viability was measured by fluorescence in the Spectra Max I3 multimode microplate reader and reported as relative fluorescence units. The IC50 values were determined by nonlinear regression using Prism GraphPad 10.

Half-maximal cytotoxicity concentration determination and selectivity index calculation

Bone marrow–derived macrophages were differentiated in vitro and cultured for 48 hours with drugs between 0.2 and 150 μM. Alamar blue was added, and viability was assessed for 18 hours following the manufacturer's instructions to define half-maximal cytotoxicity concentration. The selectivity index was calculated as follows:

$$\frac{\text{IC50 of macrophages}}{\text{IC50 of metacyclic parasites}}$$

Half-maximal effective concentration determination using high-content microscopy

The half-maximal effective concentration, 50% of the effective concentration to induce maximal killing of the parasites in infected cells, was measured by high-content microscopy. A total of 7×10^5 bone marrow–derived macrophages were infected with *Leishmania major* mCherry or *L major* Sd-RFP at multiplicity of infection of 10 in complete RPMI. After 3 hours, nonphagocytosed parasites were washed away at room temperature. Twenty-four hours after infection, the drugs were added at a concentration of 3.7, 7.5, 15, and 30 μM in supplemented RPMI, and a group without drugs was kept as a control. After 48 hours of treatment, cells were fixed with 4% paraformaldehyde; permeabilized with 0.1% PBS-Tween for 10 minutes; washed with PBS; and then blocked with 3% milk, 0.01% sodium azide, and 0.5% triton x-100 for 30 minutes. To amplify the fluorescent signal intensity of parasites, cells were stained for 1 hour with primary antibody Rabbit Anti-RFP, followed by secondary Donkey anti-Rabbit Alexa 555–coupled (Invitrogen) antibody. Nuclei were stained with DAPI for 1 hour. Cells were washed and processed with ImageXpress Micro C (confocal) high-content Imaging system XLS from Molecular Device LLC. Cell and parasite numbers were counted using an automated software program (MetaExpress) (Eren et al, 2018).

Bone marrow–derived dendritic cell in vitro experiment

Bone marrow–derived dendritic cells were cultured in complete RPMI in 12 well plates (4×10^5/ml). Three hours after culture, metacyclic *Leishmania* species were added at multiplicity of infection of 10, and 30 μM ACB1801 were added. To analyze aryl hydrocarbon receptor signaling, *Leishmania*-infected dendritic cells were treated with 1 μM of GNF351 (aryl hydrocarbon receptor antagonist, HY-102023), 0.5 μM of GNF-PF3777 (IDO2 antagonist, HY-100687), and 3 μM of PF06840003 (IDO1 antagonist, HY-101111), all from MedChemExpress. For aryl hydrocarbon receptor activation, bone marrow–derived dendritic cells were infected with *L major* Seidman at multiplicity of infection of 10 and 3 hours after infection. A total of 30 μM of ACB1801 and FICZ (HY-12451), from MedChmExpress, was added at different concentrations (0.4, 2, and 10 nM). The costimulatory molecule expression was further analyzed by flow cytometry 24 hours after infection and analyzed using Flowjo, version 10.

RNA sequencing

The MERCURIUS BRB-seq libraries were prepared for sequencing at Alithea Genomics Laboratory (Epalinges, Switzerland). In brief, RNA samples were shipped on dry ice and underwent quality control assessment. The reverse transcription was performed using barcoded oligo-dT primers. The resulting cDNA from each sample was pooled into a single tube before proceeding to cDNA second strand synthesis.

To generate Illumina-compatible libraries, the Unique dual-indexed library preparation method was employed following the previously described protocol (Alpern et al., 2019). Subsequently, the libraries were sequenced on the Illumina NovaSeq instrument at the average depth of 12 M reads per sample.

The resulting FASTQ files were sample demultiplexed and aligned to the reference genome using STARsolo, version 2.7.9a. The resulting count matrices were further utilized for downstream gene expression analysis.

Differentially expressed gene analysis was performed using DESeq2, version 3.15 (Love et al., 2014). Log_2 fold change ranked gene list by comparing ACB1801-treated samples to vehicle-treated samples was used for gene set enrichment analysis, which was conducted using clusterProfiler, version 3.17, with the default settings (Yu et al., 2012). The gene set database (version msigdb.v2023.1.Hs.entrez) was downloaded from www.gsea-msigdb.org (Subramanian et al., 2005) The conversion of murine gene Ensemble identifications to human Entrez identifications was performed with the biomaRt package, version 2.46.3 (Durinck et al., 2009, 2005) using reference mart https://dec2021.archive.ensembl.org.

The plots were produced using R packages clusterProfiler and ComplexHeatmap, version 2.12.1 (Gu et al., 2016).

Flow cytometry analysis

Stained cells were analyzed using LSR-Fortessa (BD Bioscience) and analyzed with FloJo software (version 10). The following antibodies were used to detect cell surface expression: anti–CD45-BUV737 (clone 30_F11, eBioscience), anti–CD11b-BV605 (clone M1/70, eBioscience), anti–Ly6G-allophycocyanin (APC)-cy7 (clone 1A8, BioLegend), anti–Ly6C-FITC (AL-21, eBioscience), anti–CD11c-AF700 (N418, eBioscience), anti–F480-APC (BM8, BioLegend), major histocompatibility complex class II-AF700 (M5/114.15.2, eBioscience), anti–CD40-FITC (1C10, eBioscience), anti–CD86-BV605 (GL1, eBioscience), anti–PDL1-BV786 (B7-H1, eBioscience), arginase-AF700 (A1exF5, eBioscience), nitric oxide synthase-APC (CXNFT, eBioscience), anti–CD4-

AF700 (RM4-5, BioLegend), and anti−CD8-APC (53-6.7, Biolegend). For intracellular staining, cells were stimulated for 4 hours at 37 °C with 50 μg/ml phorbol myristate acetate, 500 μg/ml ionomycin, and 1 μg/ml GolgiPlug (BD Bioscience). Cells were stained first for extracellular markers and live/dead dye and fixed with 2% paraformaldehyde. FoxP3 permeabilization kit (eBioscience) was used to permeabilize the cells. Then, cells were stained for 45 minutes with intracellular cytokines. The following intracellular markers have been used: Anti−IFN-γ-PeCy7 (XMG1.2, BioLegend), anti−IL4-FITC (eBioscience), anti−IL10-phycoerythrin (eBioscience), anti−FoxP3-Percep Cy5.5 (BioLegend), and anti−TNF-α-APC Cy7 (eBioscience).

SUPPLEMENTARY REFERENCE

Eren RO, Kopelyanskiy D, Moreau D, Chapalay JB, Chambon M, Turcatti G, et al. Development of a semi-automated image-based high-throughput drug screening system. Front Biosci (Elite Ed) 2018;10:242−53.

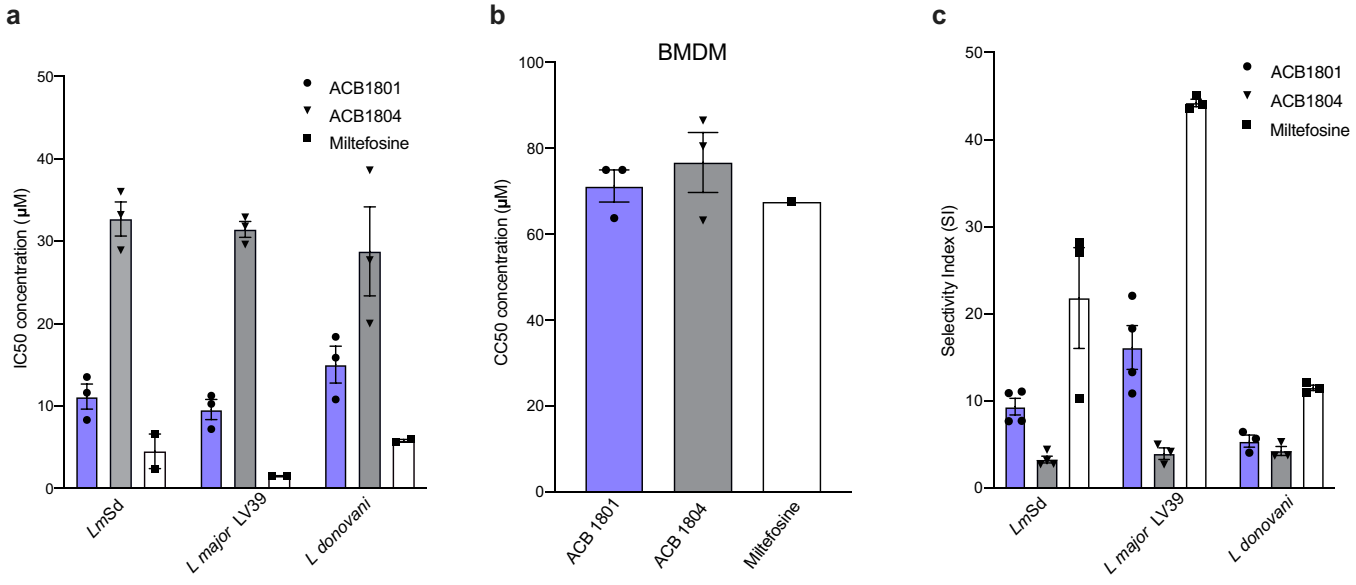

Supplementary Figure S1. Direct effect of ACB drugs on *Leishmania* and macrophages. (**a**) Summary of IC50 of 3 strains of *Leishmania* treated with ACB1801, ACB1804, and miltefosine using Alamar blue. (**b**) CC50 in macrophages. BMDMs incubated for 48 h with a serial dilution of ACB1801, ACB1804, and miltefosine and CC50 were determined by Alamar blue. (**c**) Selectivity index was calculated by dividing CC50 by IC50. ACB, β-carboline derivative; BMDM, bone marrow−derived macrophage; CC50, half-maximal cytotoxicity concentration; h, hour; IC50, half-maximum inhibitory concentration.

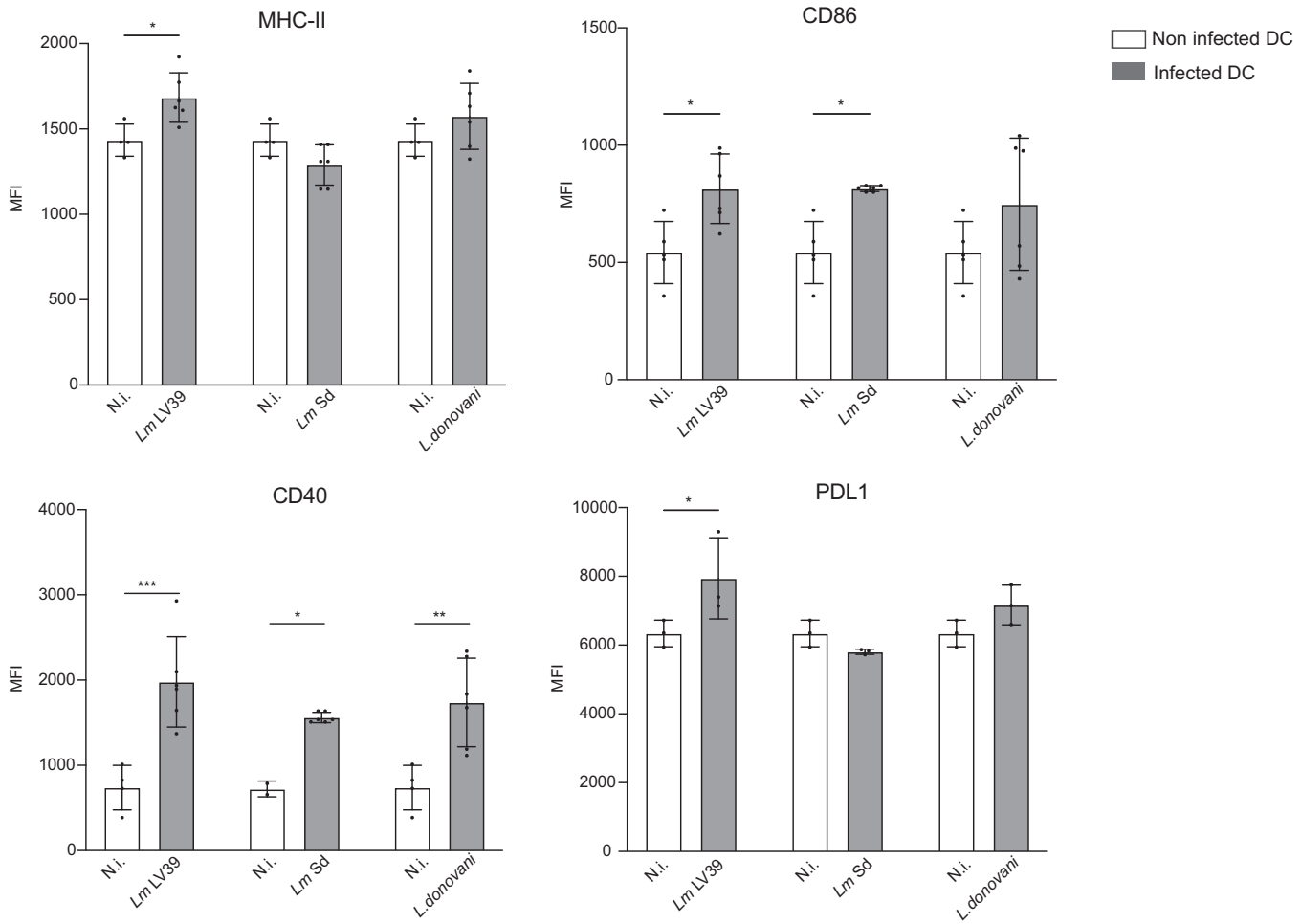

Supplementary Figure S2. MHC-II and costimulatory molecules expression on noninfected and *Leishmania*-infected DCs. **(a)** A total of 4 × 105 BMDCs were infected with *Lm*Sd, *L major* LV39, and *L donovani* metacyclic promastigotes at a MOI of 10. MHC-II and costimulatory molecule expressions were analyzed by flow cytometry 24 h later. Results are presented as MFI. Results are 1 representative experiment of 3. Data are presented as mean values ± SEM. *P*-values were calculated using 2-way ANOVA compared with vehicle-treated mice. N.i. denotes not infected DCs, and Lm LV39 denotes *L major* LV39. BMDC, bone marrow–derived dendritic cell; DC, dendritic cell; h, hour; LmSd, *Leishmania major* Seidman; MFI, mean fluorescence intensity; MHC-II, major histocompatibility complex class II; MOI, multiplicity of infection.

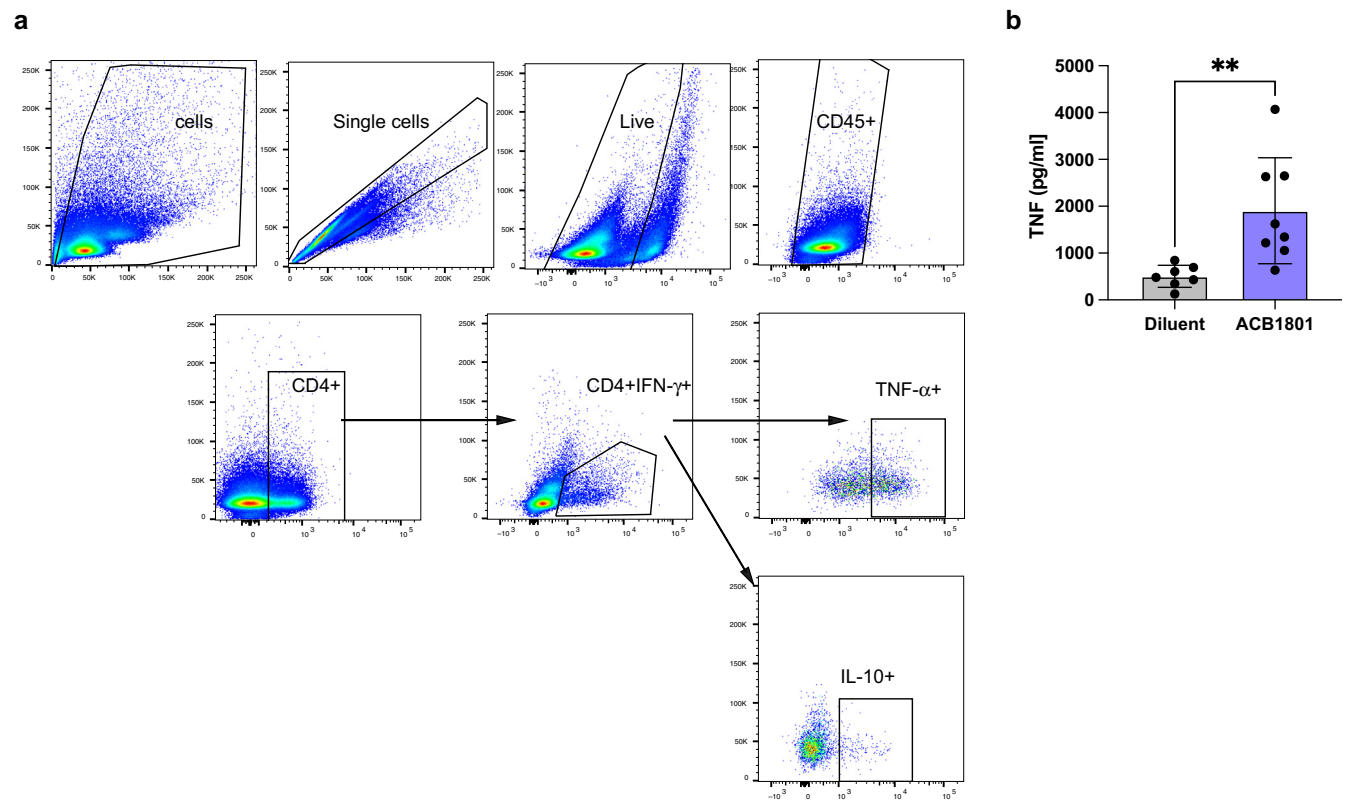

Supplementary Figure S3. Gating strategy to analyze adaptative immune response in ACB1801-treated mice. **(a)** *Lm*Sd-infected mice were treated from day 12 p.i. and killed after 10 days of treatment. Gating strategy for identification of CD4+ cells producing TNF-α or IL-10 in dLNs. **(b)** Quantification of TNF-α after restimulation of dLN cells in the presence of UV-killed LmSd (72 h) by ELISA. The data are from a pool of 2 independent experiments. Mann–Whitney test was used. $*P < .05$ and $****P < .0001$. dLN, draining lymph node; h, hour; LmSd, *Leishmania major* Seidman; p.i., postinfection.

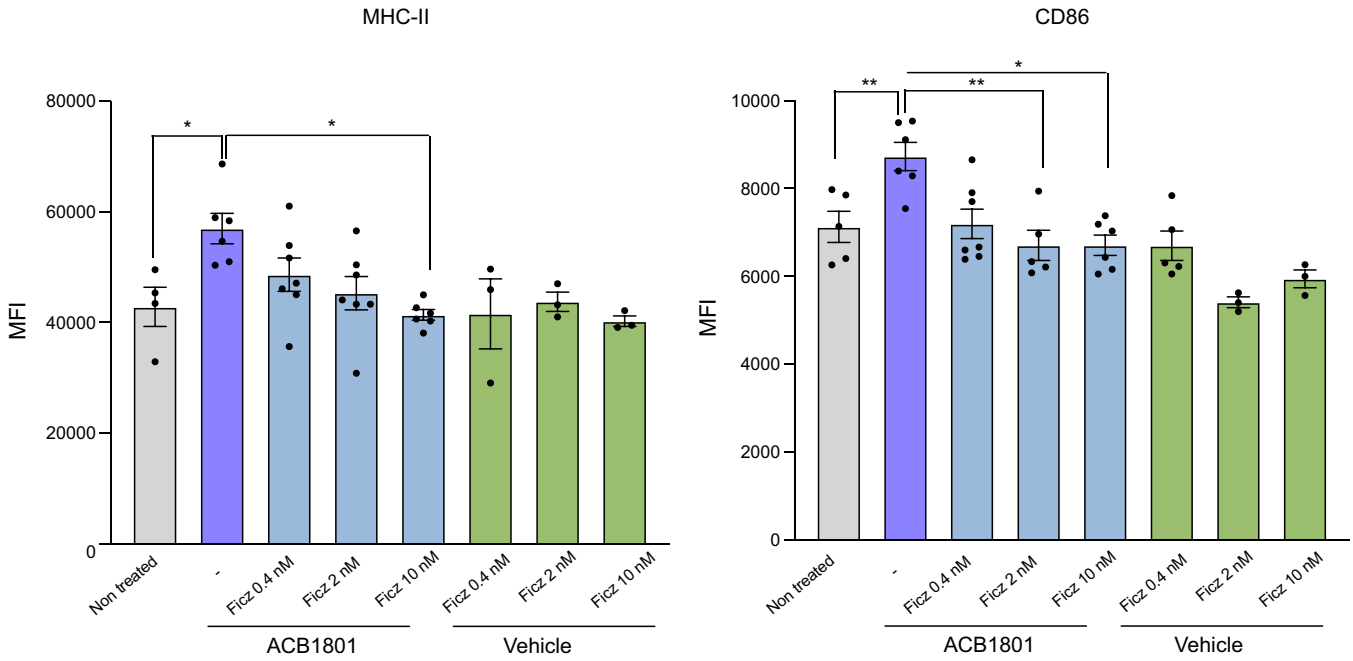

Supplementary Figure S4. Dose-dependent effect of AhR activator on immunomodulatory effects of ACB1801. A total of 4 × 105 BMDCs were infected with *Lm*Sd metacyclic promastigotes at a MOI of 10. Three hours after infection, ACB1801 was added in the presence or not of the indicated increasing doses of the FICZ AhR activator. MHC-II and CD86 cell surface expression was analyzed by flow cytometry 24 h after infection. Data are from 1 representative experiment of 3 independent experiments with 4 technical replicates per condition. K denotes thousand. AhR, aryl hydrocarbon receptor; BMDC, bone marrow–derived dendritic cell; h, hour; LmSd, *Leishmania major* Seidman; MHC-II, major histocompatibility complex class II; MOI, multiplicity of infection.